Original

De Leon, A.S.; Malhotra, S.; Molina, M.; Calderon, M.; Munoz-Bonilla, A.; Rodriguez-Hernandez, J.:

Fabrication of honeycomb films from highly functional dendritic structures: electrostatic force driven immobilization of biomolecules

In: Polymer Chemistry (2016) Royal Society of Chemistry

DOI: 10.1039/C6PY00601A

Polymer Chemistry

PAPER

View Article Online
View Journal | View Issue

Cite this: *Polym. Chem.*, 2016, **7**, 4112

Fabrication of honeycomb films from highly functional dendritic structures: electrostatic force driven immobilization of biomolecules

A. S. De León,[a] S. Malhotra,[b] M. Molina,[b] M. Calderón,[b,c] A. Muñoz-Bonilla*[d] and J. Rodríguez-Hernández*[a]

Received 5th April 2016,
Accepted 22nd May 2016

DOI: 10.1039/c6py00601a

www.rsc.org/polymers

Herein we report the preparation of honeycomb porous films for selective immobilization of biomolecules *via* the breath figure technique, a water-assisted micropatterning method. In particular, porous films are obtained from polymeric blends composed of high molecular weight polystyrene as the major component and an oligoglycerol based dendron covalently bonded to a hydrophobic polystyrene chain as the minor constituent. The multivalent dendritic architecture presents a well-defined molecular structure with controlled glycine arrays on their surfaces. Due to the mechanism of the breath figure formation, the resulting films exhibit an especial chemical distribution at the surfaces, in which the dendritic functional polymer is located preferentially in the interior of the pores while the rest of the polymer surface is mainly formed by the high molecular weight polystyrene. The high amount of amine functional groups inside the pores allowed the specific immobilization of biomolecules into the cavities by electrostatic interactions. In particular, the protein bovine serum albumin (BSA) and a DNA sequence were attached onto the films as a proof of concept. Besides, it was demonstrated that the density of biomolecules immobilized can be easily tuned by varying the content of the dendritic functional polymer in the film. These unique characteristics open new alternatives for the use of these platforms in biorelated applications including bio-recognition processes, or the understanding of cell–protein and even cell–DNA interactions on biofunctional microstructured polymeric supports.

Introduction

The preparation of porous materials with well-defined pore size and narrow size distribution has been extensively studied during the last decade. The interest in the elaboration of such materials relies on their multiple applications which are of potential interest. Some examples include their use as catalytic supports,[1] gas absorbents,[2] filtration membranes[3–5] or for their interesting optical properties[6] in those porous films with the appropriate pore size. Moreover, a large amount of work has been devoted to the preparation of porous films for biorelated purposes. This group of applications includes their use as biosensors[7] and as supports for cell culture[8] or for biorecognition purposes.[9,10]

Different alternatives have been developed to prepare well defined porous films. These involve the use of templates such as ordered arrays of colloidal particles to produce inverse opal structures,[6,7,11,12] natural biological templates,[13] from transformed polymeric sphere arrays[14,15] using emulsion droplets as templates[16] by thermally induced phase inversion[17] or self-organized surfactants,[18] among others.

In this context, the breath figures (BFs) approach is one of the most extended methodologies for overcoming several major drawbacks of the above mentioned methodologies.[19,20] First of all, porous films can be obtained in one single step in a very fast process (from few seconds up to 2 minutes). Second, in the breath figures approach water acts as a template and can be thus easily removed by simple evaporation. Finally, the use of polymer blends permits one to modify the chemistry of the pores as well as the distribution of the blend components on the film surface.

Most of the biorelated applications require the immobilization of biomolecules on the material surface. For instance, the immobilization of biomolecules such as DNA on surfaces is a current research topic due to its many applications, par-

[a]*Instituto de Ciencia y Tecnología de Polímeros (ICTP), Consejo Superior de Investigaciones Científicas (CSIC), C/Juan de la Cierva 3, 28006 Madrid, Spain. E-mail: jrodriguez@ictp.csic.es*
[b]*Freie Universität Berlin, Institute of Chemistry and Biochemistry, Takustr. 3, 14195 Berlin, Germany*
[c]*Helmholtz Virtuelles Institut – Multifunctional Biomaterials for Medicine, Helmholtz-Zentrum Geesthacht, Kantstr. 55, 14513 Teltow, Germany*
[d]*Departamento de Química-Física Aplicada, Facultad de Ciencias, Universidad Autónoma de Madrid, C/Francisco Tomás y Valiente 7, Cantoblanco, 28049 Madrid, Spain*

ticularly in the development of bio-based devices, including sensors, microarrays or transistors.[21–23] Besides, in implantable materials, their biocompatibility, performance and efficacy are directly related to the functionality of the interfaces that govern different processes including cell adhesion and proliferation.[24]

Some groups resorted to the attachment of many different biomolecules through the functional moieties present at the interface. In contrast, others incorporated the biomolecule into the polymeric solution and prepared the films by casting.[25] The latter led, in the reported procedures, to a homogeneous distribution of protein over the entire material. However, in some cases, a particular biomolecule distribution as well as adjusting the biomolecule density present at the surface are key aspects that require to be controlled.[26] In particular, adhesion, migration and proliferation events are directly related to the control over the geometrical area, spacing between the functional groups and the density of active biomolecules.[27]

In the literature, low molecular weight (LMW) dendron based architectures were successfully synthesized and evaluated among others for their potential in biology-related applications.[28,29] In this context, we have recently shown that using oligoglycerol based dendrons, it is possible to enhance multivalent interactions for drug and gene delivery.[30–32] Oligoglycerol based dendrons with their tree-like structure and large number of hydroxyl end-groups serve as a hydrophilic part within an amphiphilic structure. Their water solubility and physiological safety, which is based on the very biocompatible glycerol building block, together with minimum non-specific interactions with proteins, has the potential for use in biomedical applications.[33,34] Also, chemical post-modifications offer excellent opportunities for multivalent interactions with biological substrates, which resulted in considerably stronger binding affinities compared to monovalent interactions. In addition, the degree of branching and thus flexibility can be varied by choosing a certain dendron generation.[35]

In this manuscript, we describe the immobilization of two different biomolecules, *i.e.* a model BSA protein and DNA by using electrostatic forces between the positively charged groups of the oligoglycerol dendrons present at the pore surface and those oppositely charged moieties present in the structure of the biomolecule. The positively charged groups will be obtained by using homopolystyrene (PS) modified with a positively charged oligoglycerol based dendritic structure having multiple primary amine functional groups per macromolecule. This fact will permit, in principle, a high functionalization degree as well as a control over the pore size and distribution at the surface of the film. Moreover, the strategy proposed will allow us to control the biomolecule density present at the surface as well as their position and distribution at the interface. Finally, we describe non-covalent immobilization of biomolecules exclusively at the pore surfaces while the rest of the film remains unmodified. Non-covalent biomolecule immobilization is currently being evaluated in order to deliver proteins and DNA into cells attached to the surface.

Experimental section

Materials

Sodium azide (NaN_3, 99.5%, Sigma-Aldrich), trifluoroacetic acid (99%, Sigma-Aldrich), copper(I) bromide (CuBr, 99.999%, Aldrich), *N*,*N*,*N*′,*N*″,*N*″-pentamethyldiethylenetriamine (PMDETA, 99%, Aldrich), (2-bromoethyl)benzene (98%, Sigma-Aldrich), chloroform ($CHCl_3$, Scharlau), dichloromethane (CH_2Cl_2, Scharlau), tetrahydrofuran (THF, Scharlau), dimethylformamide (DMF, anhydrous, 99.8%, Alfa-Aesar) and methanol (MeOH, Scharlau) were used as received. High molecular weight polystyrene (PS, Aldrich, M_w = 2.5 × 10^5 g mol^{-1}) was used as a polymeric matrix. Round glass coverslips of 12 mm diameter were purchased from Ted Pella Inc. Regenerated cellulose dialysis tubing (Cellu-Sep T1 with a cut-off molecular weight of 1.0 and 3.5 kDa) was purchased from Membrane Filtration Products Inc., Seguin, Texas. FITC labeled bovine serum albumin (BSA-FITC) was received from Life Technologies and the DNA sequence (5′-CTGGACTTCCAGAAGAACATT-3) from Operon Biotechnologies GmbH.

Synthesis of (a) PS_{35}-Br and end-modification to (b) PS_{35}-N_3 azide

PS_{35}-Br was obtained by atom transfer radical polymerization (ATRP) using previously reported procedures (M_n = 3700 g mol^{-1}, M_w/M_n = 1.11) using phenylethyl bromide as an initiator.[9] Then the PS_{35}-Br polymer reacted with NaN_3 (10 fold excess) in DMF at room temperature for 24 h to displace the labile Br group by an azide able to further react with the alkyne group of the dendrons *via* click chemistry. Successful quantitative displacement was observed by ^{1}H-NMR.

Synthesis of alkyne functionalized dendrons

Alkyne functionalized dendrons both protected (Dp-alk) and deprotected (Ddp-alk) were synthesized following the previously published procedures[30,36] and characterized by ^{1}H-NMR. (c) Dp-alk: ^{1}H NMR (400 MHz, methanol-d_4): δ 1.42 (36H, brs, –OC(CH_3)$_3$), 2.82–2.84 (1H, m, –CC*H*), 3.50–3.58 (15H, m, PG-dendron), 3.67 & 3.80 (2 × 4H, 2s, –CO–CH_2–NHBoc), 4.30–4.31 (2H, d, J = 2.4 Hz, HCC–CH_2–O); HRMS: *m*/*z* Calcd: $C_{40}H_{66}N_4NaO_{19}^+$: 929.4200; found: 929.4192. (d) Ddp-alk: ^{1}H NMR (400 MHz, methanol-d_4): δ 2.84 (1H, s, –CC*H*), 3.69–3.72 (12H, m, PG-dendron), 3.61 (3H, brs, PG-dendron) 3.87 & 3.89 (2 × 4H, 2s, –CO–CH_2–NH_2), 4.29–4.31 (2H, m, HCC–CH_2–O); HRMS: *m*/*z* Calcd: $C_{20}H_{34}N_4NaO_{11}^+$: 529.2100; found: 529.2120.

Synthesis of the polystyrene-*b*-dendron block copolymer

The azide terminated PS macroinitiator (PS-N_3) was allowed to react with both, Dp-alk and Ddp-alk. A click reaction was performed following the conditions of a classic ATRP reaction.[37] In particular, Dp-alk (25.0 mg, 0.034 mmol), PS-N_3 (42.8 mg, 0.012 mmol), PMDETA (1.5 mg, 0.009 mmol) and CuBr (0.8 mg, 0.009 mmol) were mixed in 0.7 mL of dry DMF under an argon atmosphere. Similarly, Ddp-alk (105.2 mg, 0.116 mmol), PS-N_3 (145.1 mg, 0.041 mmol), PMDETA (5.0 mg, 0.029 mmol), and CuBr (2.9 mg, 0.029 mmol) were mixed in

1.0 mL of dry DMF under an argon atmosphere. In both cases, a fixed molar proportion of alkyne : azide : PMDETA : CuBr of 4 : 1.4 : 1 : 1 was maintained and the reaction proceeded for 24 h at room temperature. The success of the reactions was followed by Fourier transform infrared (FTIR) and ^{1}H-NMR. The product obtained from the click reaction of the unprotected dendron (PS-Ddp) was purified by precipitation in cold MeOH and then dried in a vacuum. The product obtained from the click reaction of the protected dendron (PS-Dp) was dialyzed inside a membrane of 3.5 kDa against water and then lyophilized. Then, deprotection of the BOC groups of the dendron was carried out by using a 1 : 3 mixture of trifluoroacetic acid and CH_2Cl_2 at room temperature overnight. The solvent was then evaporated under vacuum and redissolved in THF prior to dialysis against water in a 1 kDa membrane. The product was observed to precipitate during the dialysis process. Finally, the product was lyophilized.

Film preparation of the porous films by the breath figures technique

Different blends were studied by varying the total concentration of polymers in chloroform solutions (15, 30 and 70 mg mL^{-1}) and the proportion of PS-Ddp (5, 10 and 20 wt%) and linear PS (95, 90 and 80 wt%) in each of the polymer solutions. Films were prepared from these solutions by casting 60 ml onto 1.2 cm (in diameter) glass wafers at room temperature at 98% relative humidity (RH) inside a closed chamber. The humidity was controlled by introducing water reservoirs and allowing the humidity to reach the water vapor at the equilibrium. At room temperature relative humidities of around 98–99% can be obtained overnight. The glass supports were used as received upon extensive washing with water and subsequently with ethanol.

Characterization

^{1}H-NMR and ^{13}C-NMR analyses were performed in a Bruker 300 MHz NMR spectrometer using either deuterated chloroform or water as the solvent. FTIR spectra were recorded using a Perkin Elmer Spectrum One. Scanning electron microscopy (SEM) measurements were performed in a Philips XL30 with an acceleration voltage of 25 kV. The samples were coated with gold–palladium (80/20) prior to scanning. Fluorescence microscopy was performed using a Leica DMI-3000-B fluorescence microscope. Images were acquired using different magnifications (×10 and ×40) and the corresponding set of filters for imaging green fluorescence and bright field.

Results and discussion

In this manuscript, we describe the preparation of regular honeycomb films using a polystyrene-*b*-dendron block copolymer with amine terminal groups. This structure combines the presence of polar moieties with branched ends and appears in principle, to be an excellent candidate for producing well-defined porous films according to the literature.[38,39] On the one hand, the pioneer studies of Francois and others carried out later suggested that branched structures can enhance the order of the porous films. Equally, polar functional groups incorporated into the polymer structure stabilized the condensed water droplets, thus preventing them from coagulation.[19,20]

The structure of the polystyrene-*b*-dendron block copolymer (PS-Ddp) as well as the two alternative preparation routes is depicted in Scheme 1. The first step involves the synthesis of PS with controlled molecular weight and narrow polydispersity. We resort to atom transfer radical polymerization (ATRP) to achieve this goal with the preparation of the PS_{35}-Br polymer (M_n = 3700 g mol^{-1}, M_w/M_n = 1.11). In the second step, the bromide end functional group of the PS was modified to introduce the azide moiety, which will serve to anchor the alkyne-modified dendron. This reaction was carried out using a large excess of NaN_3 to ensure a high modification degree of the end group with the formation of PS-N_3. As depicted in Fig. 1, the FTIR

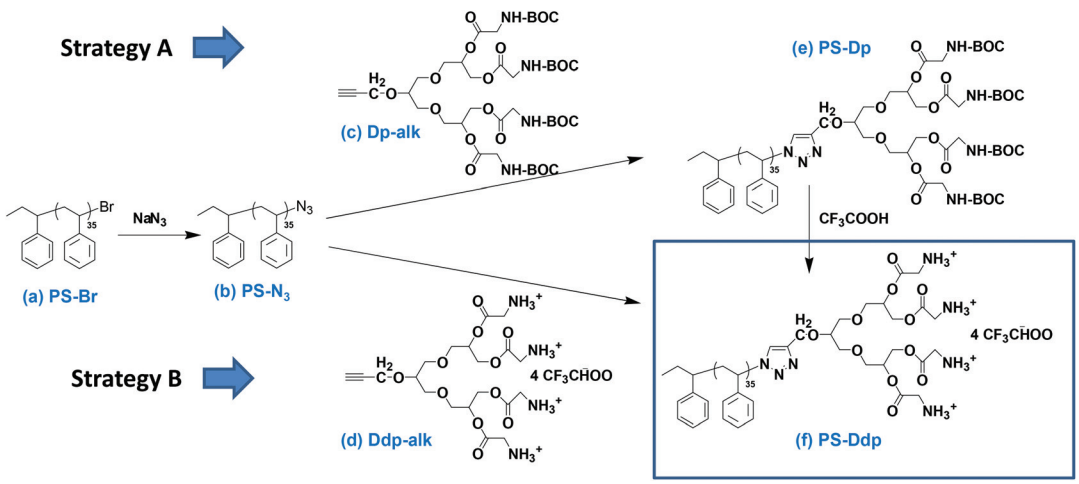

Scheme 1 Synthetic approaches used for the preparation of a polystyrene-*b*-dendron block copolymer *via* click chemistry between an azide modified PS and an alkyne functional dendron.

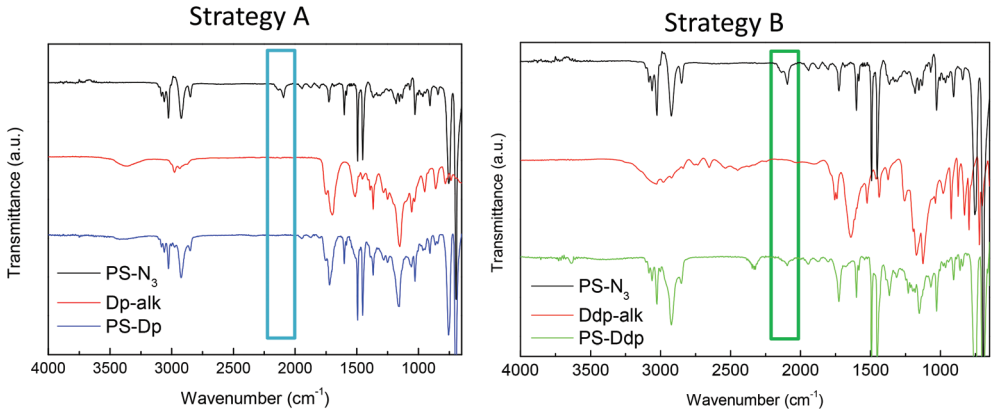

Fig. 1 FTIR spectra of the different precursors of polystyrene-*b*-dendrons: PS-N_3: azide end-functionalized PS, Dp-alk: dendron protected, Ddp-alk: dendron deprotected. In each graph, the FTIR spectrum below stands for the final product, *i.e.* PS-Ddp.

spectrum indicates the formation of an azide group evidenced by the presence of a signal at ~2100 cm^{-1}. NMR measurements also confirmed the success of the reaction. In Fig. 2 the signal at 4.35–4.65 ppm corresponding to the methine proton neighboring the bromine chain end completely shifts to 3.84–4.1 after the reaction with NaN_3 due to the substitution of the bromine by azide moieties.[40]

The final step in the preparation of PS-Ddp involves the coupling reaction *via* click chemistry with the alkyne modified dendron. At this stage two different alternatives were explored. On the one hand, in **Strategy A** the click reaction was carried out using a dendron having the amino groups protected with a *tert*-butyl group (Dp-alk). This route requires a second step to remove the protective groups. On the other hand, the possibility to carry out the click chemistry reaction using the amino-deprotected dendron (Ddp-alk) directly was explored in **Strategy B**. Independently of the approach employed, the click reaction, typically carried out in aqueous solution, was performed in this study using DMF in order to dissolve all the components. More precisely, this reaction was accomplished by using PMDETA and CuBr in stoichiometric amounts, conditions typically used in ATRP,[41] and using an excess of the dendron. The characterization of these products obtained from both dendrons was first achieved by FTIR as depicted in Fig. 1. As can be observed in both graphs the success of the reaction can be evidenced following the azide signal that appears at ~2100 cm^{-1}. **Strategy A** involves the use of the protected dendron, and the azide signal completely disappeared during the reaction. As expected, the azide group is transformed into triazole during the coupling reaction. On the other hand, **Strategy B** carried out using the deprotected dendron permits the preparation of the final polystyrene-*b*-dendron in one single step. However, as can be observed in Fig. 1, the spectrum of the final product after the click chemistry reactions presents a small band corresponding to the unreacted azide group. This indicates that the reaction has been only partially accomplished. The amount of transformed azide functional groups can be estimated using the aromatic PS signal as the reference. As a result, only 62% of the azide precursor successfully reacted with the alkyne modified dendron. Most probably, the primary amine groups interact with the catalyst, thus limiting the conversion of the reaction.

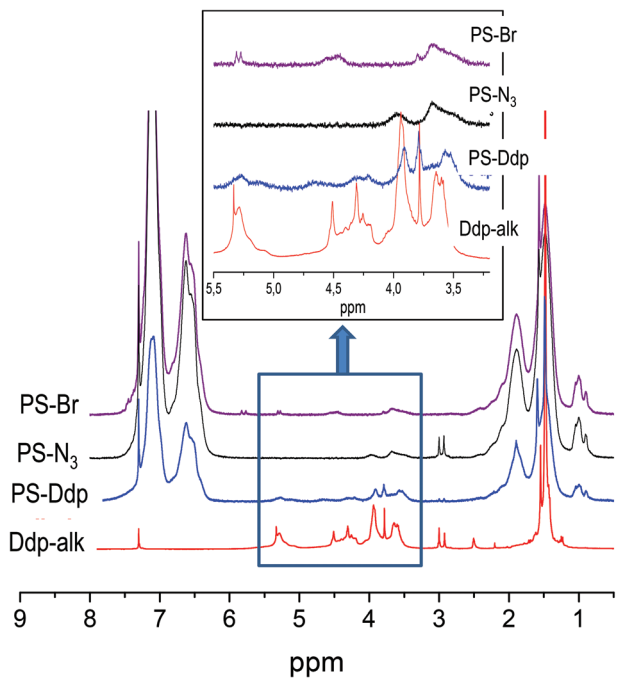

Fig. 2 ^{1}H-NMR spectra of the functional polystyrenes PS-Br, PS-N_3, PS-Ddp and the dendron with protected amino functional groups, Ddp-alk in $CDCl_3$.

Based on this finding, **Strategy A** was selected for the preparation of the PS-Ddp additive to be used in the formation of the breath figures structures. In addition to FTIR, ^{1}H-NMR can provide further information about the chemical integrity of the product. In Fig. 2, the ^{1}H-NMR spectra of the precursors as well as the product of the coupling click reaction are depicted. As expected, the ^{1}H-NMR spectrum of the resulting product

(PS-Ddp) contains the aromatic signals, between 6.2 and 7.5 ppm, provided by the PS as well as those signals from the dendron both in the region of 3.5–5.5 ppm corresponding to the –CH- and –CH_2- groups and the signal at ~1.5 ppm associated with the *tert*-butyl protective groups. The presence of these signals clearly indicated the success of the coupling reaction.

Upon hydrolysis of the *tert*-butyl groups following already reported procedures, the dendron with the primary amine functional groups was finally obtained, PS-Ddp. Basically, deprotection involves the use of trifluoroacetic acid (TFA) in chloroform at room temperature. Once the deprotected polystyrene-*b*-dendron block copolymer was successfully synthesized, it was then employed as an additive in a polymeric matrix of PS for the preparation of porous films by the breath figures approach, a method that involves simple solvent casting under moist conditions.

The environmental conditions were identical for all the experiments: saturated vapor conditions and room temperature. The first series of experiments were conducted to determine the role of the functionality as well as the dendritic nature of the additive on the regularity of the pattern. In Fig. 3 are shown the resulting porous films prepared from the blends of 90 wt% of the PS matrix and 10 wt% of either the azide end-functionalized PS or the polystyrene-*b*-dendron block copolymer, using two different total polymer concentrations, *i.e.* 30 mg mL^{-1} and 70 mg mL^{-1}. As is observed, independently of the concentration employed the branched structure leads to a regular array of pores having similar sizes and exhibiting a hexagonal array. On the contrary, the films prepared using azide-terminated polystyrene (PS-N_3) did not show the same order and produced rather irregular arrays. These findings corroborate that a dendritic structure with multiple functional groups with high water affinity favors the formation of a regular porous pattern.

The use of this type of macromolecule (PS-Ddp) as an additive instead of a classical water-soluble amphiphilic dendron (*i.e.* the same dendron but with a C12 or C18 tail, as previously reported by our group[42]) presents two additional reasons. First, the presence of a rather large hydrophobic PS block pre-

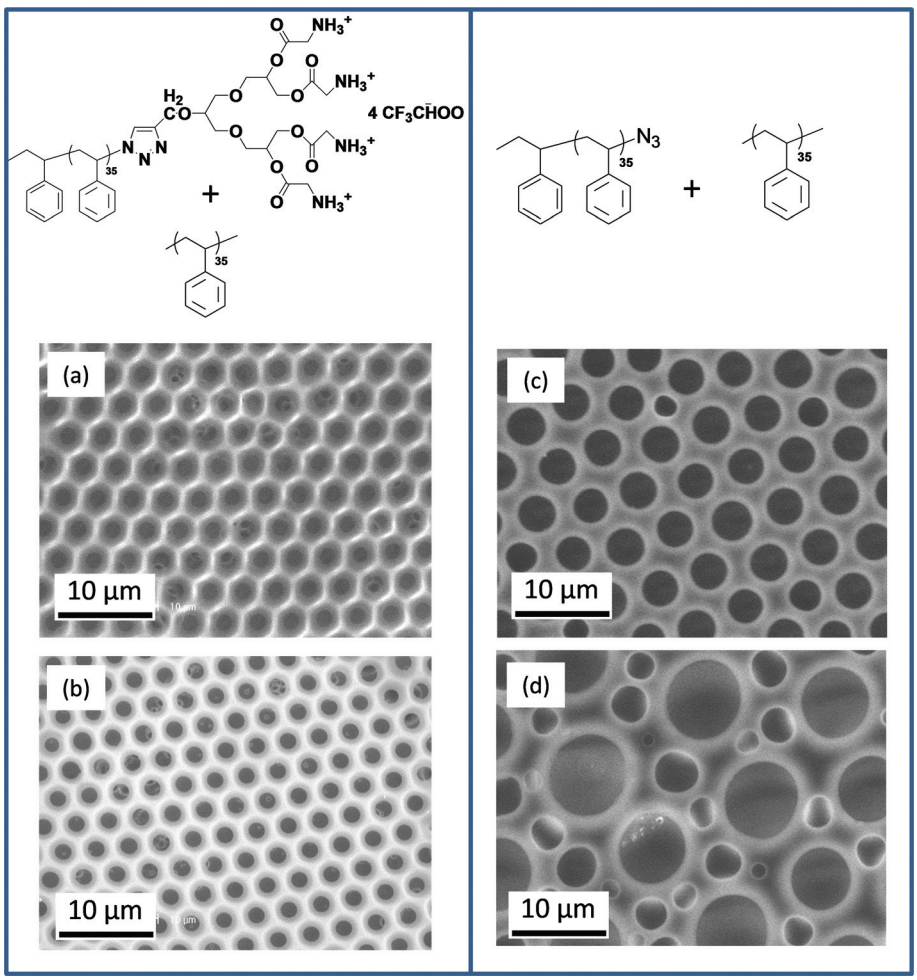

Fig. 3 Scanning electron microscopy images obtained for two different blends composed of 90 wt% of PS and 10 wt% of either (a and b) dendron end-functionalized PS or (c, d) azide end-functionalized PS. The films were prepared at two different polymer concentrations (a and c) 70 and (b and d) 30 mg mL^{-1} under 98% RH.

vents the block copolymer from being solubilized in water. This is crucial in terms of using these materials as templates for further bioassays. Solubility in water would imply the detachment from the pore surface thus losing functionalization. Second, this PS chain will also enhance the compatibility of the additive with the polymeric matrix (also hydrophobic PS), ensuring a typical distribution of this amphiphilic additive. Therefore, during the breath figures process, the hydrophilic groups (*i.e.* amine groups) will be selectively oriented towards the surface only inside the pores of the film.

In addition to the role of the macromolecular structure and functionality on the regularity of the porous films, the experimental conditions were varied to optimize the formation of honeycomb porous films. For this purpose, porous films were prepared at a lower polymer concentration, 15 mg mL^{-1} and compared with the sample obtained at 30 mg mL^{-1}. The amount of PS-Ddp in the blend (between 5 and 20 wt% in the initial feed) was also varied for each polymer concentration. As depicted in Fig. 4, at low polymer concentrations the films only exhibit a partial hexagonal order in comparison with those prepared at 30 mg mL^{-1} which show large-scale ordered honeycomb films. This sensitivity to the concentration of the solution was previously observed in other systems and it was attributed to the low capacity to stabilize the droplets and prevent their coalescence when using a small amount of solute.[43] More interestingly, at a concentration of 30 mg mL^{-1}, a reduction in the amount of functional PS-Ddp did not significantly affect the regularity of the pore arrays. Indeed, the pores obtained for blends containing 5, 10, and 15 wt% of PS-Ddp have very similar sizes and narrow pore size distributions (2.0 ± 0.1 μm, 1.8 ± 0.1 μm, and 1.9 ± 0.1 μm, respectively). As a result, contrary to those reported cases, in which linear functional polymers have been employed describing the loss of order upon reduction of the amount of additive in the blend, herein the branched macromolecular structure employed permits the preparation of ordered structures with a small amount of additive. This is probably due to the large content of the polar group in its macromolecular structure and can be used, as will be depicted below, to finely tune the density of the functional groups inside the pores, as the pore size is maintained constant.

Therefore, films prepared with a polymer concentration of 30 mg mL^{-1} were selected for the next experiments of bioimmobilizations because they allow the formation of highly ordered porous structures consuming relatively low amounts of polymer. Fig. 5 displays the SEM images of a film obtained at 30 mg mL^{-1} with 10 wt% of the polystyrene-*b*-dendron block copolymer, which show a large uniform area of pores indicative of highly ordered structures. Besides, in the cross-section image the formation of a single layer of pores is clearly observed.

Previous reports on the preparation of porous films using blends of two different components evidenced the presence of the hydrophilic component inside the pores whereas the rest of the surface is mainly decorated with the other component. This observation is the result of water condensation and simultaneous rearrangement of the hydrophilic groups towards the water droplet during the formation of the film. Based on this well-known process, the films prepared with PS-Ddp/PS blends are expected to have the polar end oriented towards the inner part of the pore while the rest of the film will mainly be composed of the PS matrix. Moreover, since the porous surfaces prepared using the aminated dendron are positively charged at neutral pH values, they may serve as a support to immobilize and obtain a micropatterning of different biomolecules having a net negative charge. For this purpose, the immobilization of two different biomolecules by electrostatic interactions was

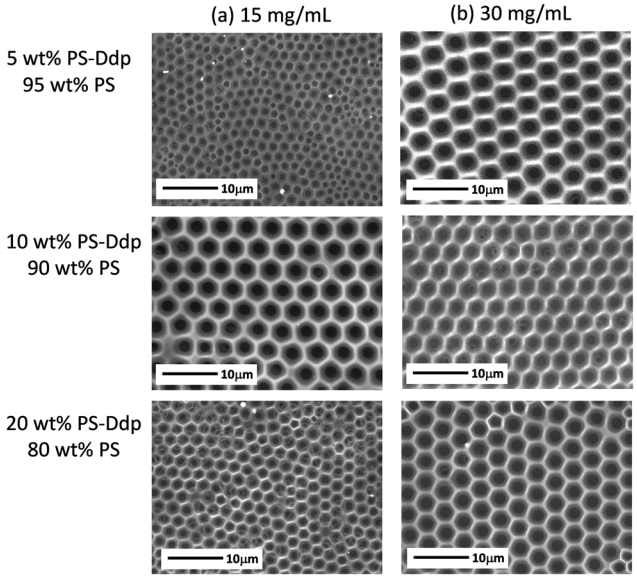

Fig. 4 SEM images of the porous films obtained using 5–20 wt% of PS-Ddp and 80–95 wt% of PS. The films were prepared at two different polymer concentrations (a) 15 and (b) 30 mg mL^{-1} varying the composition of the blend and 98% RH.

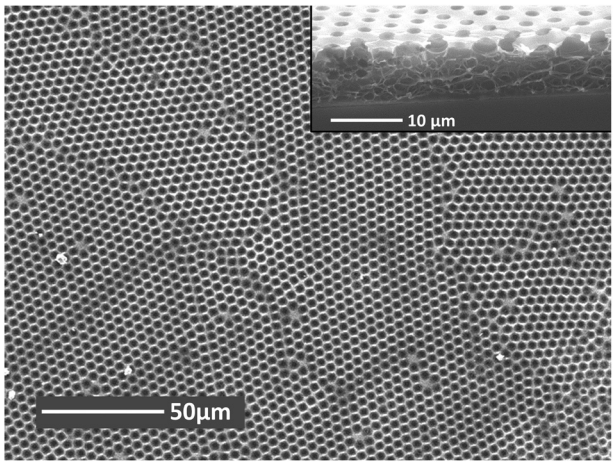

Fig. 5 Low magnification and the cross-section images obtained by SEM of the porous films prepared at a polymer concentration of 30 mg mL^{-1} using 10 wt% of PS-Ddp and 90 wt% of PS under 98% of RH.

explored. On the one hand, a fluorescent labelled protein, *i.e.* BSA-FITC having in their structure positively and negatively charged patches and with an isoelectric point at ~4.7, was employed.[44] Equally, DNA-FITC is also negatively charged at neutral pH and may be straightforwardly placed on the pores.[45] Fig. 6 shows the SEM image of a precursor film and the fluorescence images of the porous films upon incubation for 1 h with 0.1 mg mL^{-1} aqueous solution of the fluorescently labelled biomolecules, BSA and DNA. In both cases, the images revealed a fluorescent pattern corresponding to an immobilization of either BSA protein or DNA selectively inside the pore.[1] Moreover, when the same experiment is performed under the same conditions using only the PS matrix or together with PS-N_3 as the additive, no fluorescence can be

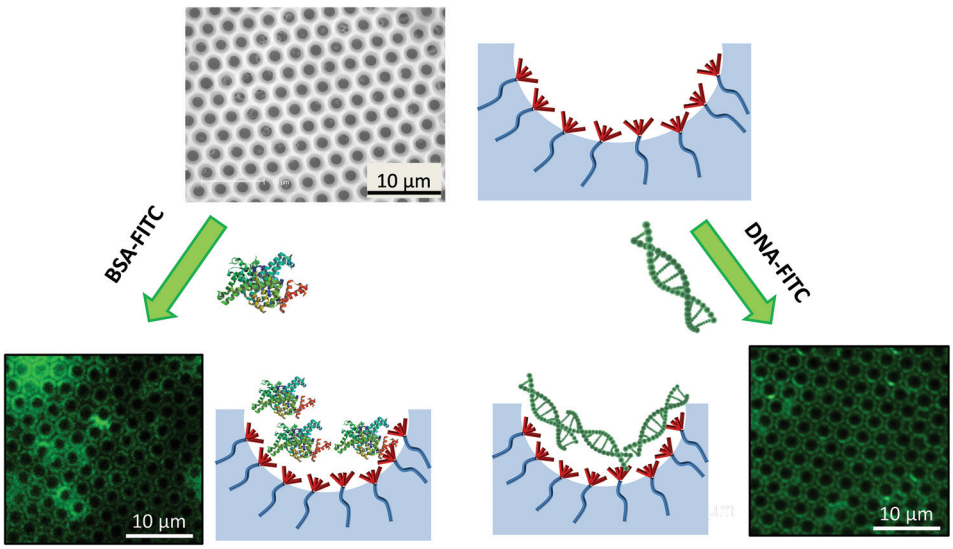

Fig. 6 Immobilization of BSA-FITC and DNA-FITC onto the porous films prepared from blends of PS-Ddp/PS 10/90 wt% in saturated vapor (polymer concentration 30 mg mL^{-1}, solvent: $CHCl_3$).

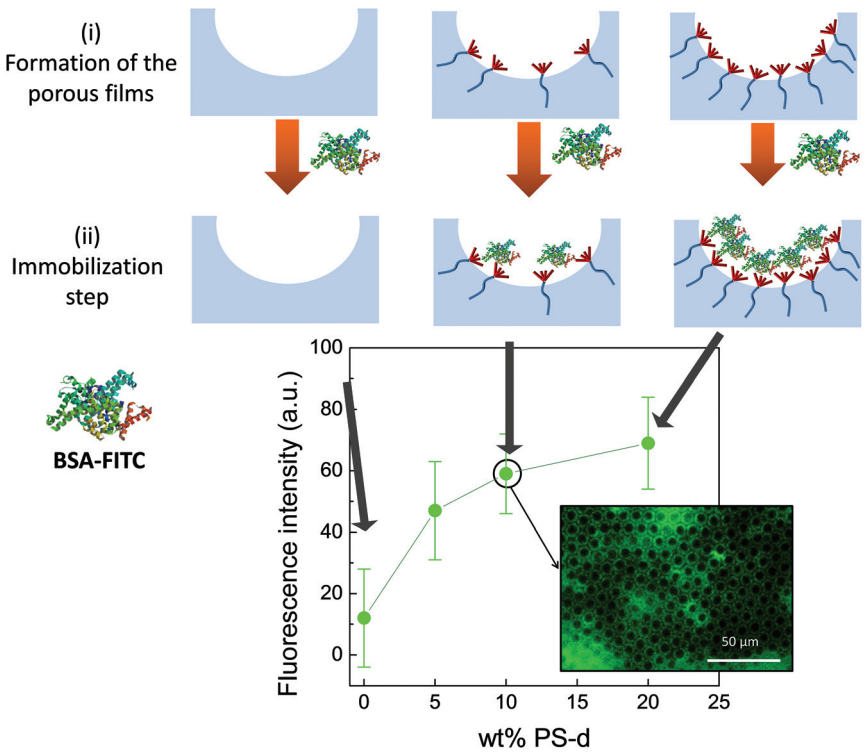

Fig. 7 Variation of the fluorescence intensity as a function of the aminated polystyrene PS-Ddp in the blend. As the amount of PS modified with the dendron employed for the blend increases, the intensity and thus the amount of biomolecules immobilized increase as well.

observed, therefore evidencing that the immobilization of the biomolecules is caused by the electrostatic interactions of the PS-Ddp located inside the pores.

In addition to the precise immobilization of the biomolecules, another advantage of using blends concerns the possibility of finely tuning the density of biomolecules immobilized. In principle, varying the amount of polystyrene-*b*-dendron block copolymer incorporated into the polymer solution would provide surfaces with pores having variable amounts of dendrons. To evaluate the possibility of modifying the amount of biomolecules immobilized, blends with variable amounts of PS-Ddp (between 5 and 20 wt%) were prepared at a polymer concentration of 30 mg mL^{-1}. Subsequently, each surface was incubated with BSA-FITC following the same conditions as aforementioned. Then, micrographs of the different surfaces were obtained by using a fluorescence microscope and the fluorescence intensity in the green channel provided by the FITC at the surfaces was analyzed by using the ImageJ software as a measure for the amount of adsorbed BSA. In Fig. 7, the obtained fluorescence intensity values are plotted *versus* the amount of PS-Ddp in the blend. A gradual increase of the fluorescence intensity is clearly observed when the blend is enriched with PS-Ddp, which indicates that a higher amount of biomolecule is immobilized. This experiment evidences indirectly that the amount of available amino groups provided by the dendron inside the pores increases by increasing the proportion of the additive in the blend. As a result, the density of functional biomolecules immobilized inside the pores that varies accordingly can be precisely tuned by taking into account the initial blend composition.

Conclusions

In summary, we report a methodology to selectively immobilize biomolecules using two different models, *i.e.* BSA protein and DNA sequences on the patterned and functionalized pores of breath figures polymer films. The process involves first, the fabrication of honeycomb films with pores enriched with amine groups. For this purpose, we demonstrated that the use of polymer blends consisting mainly of a commercial PS and a low amount (5–20 wt%) of a polystyrene-*b*-dendron block copolymer allows the formation of an ordered porous pattern in which the dendritic functional PS is mainly located inside the pores. The high amount of amine groups within the cavities due to the oligoglycerol dendritic structure permits the specific immobilization of the biomolecules through electrostatic interactions, with the formation of a biofunctional micropattern. Remarkably, the pore size of surfaces does not vary with the content of the dendritic structure in the blend, whereas the content of biomolecules progressively increases. This allows the fine control of biomolecule immobilization at the surface without the need for varying the micropattern, demonstrating the versatility of this method.

These unique characteristics open new alternatives for the use of these platforms in biorelated applications including bio-recognition processes or the understanding of cell–protein and even cell–DNA interactions on biofunctional microstructured polymeric supports. We are currently exploring the possibility of promoting surface-mediated proteins and DNA delivery that may, in turn, be internalized by the cell, *i.e.* gene delivery applications. Equally, cell transfection *in vitro* and the contact transfer and expression of DNA in vascular tissues formed on top of the surface is an aspect in which these surfaces may find interest.

Acknowledgements

This work was financially supported by the MINECO (Projects MAT2010-17016 and MAT2013-47902-C2-1-R (JRH)). A. Muñoz-Bonilla gratefully acknowledges the MINECO for her Ramon y Cajal contract. A. S. de León thanks the Ministerio de Educación for his FPU predoctoral fellowship and DAAD for his short-term scholarship for research stays (A/13/71498). M. Calderón gratefully acknowledges financial support from the Bundesministerium für Bildung und Forschung (BMBF) through the NanoMatFutur award (13N12561), the Helmholtz Virtual Institute, Multifunctional Biomaterials for Medicine and the Freie Universität Focus Area Nanoscale. M. Molina acknowledges financial support from the Alexander von Humboldt Foundation.

References

1 A. S. De Leon, T. Garnier, L. Jierry, F. Boulmedais, A. Munoz-Bonilla and J. Rodriguez-Hernandez, *ACS Appl. Mater. Interfaces*, 2015, **7**, 12210–12219.
2 L. Wu, D. An, J. Dong, Z. Zhang, B.-G. Li and S. Zhu, *Macromol. Rapid Commun.*, 2006, **27**, 1949–1954.
3 J. Mansouri, E. Yapit and V. Chen, *J. Membr. Sci.*, 2013, **444**, 237–251.
4 L.-S. Wan, J.-W. Li, B.-B. Ke and Z.-K. Xu, *J. Am. Chem. Soc.*, 2012, **134**, 95–98.
5 Y. Ou, C.-J. Lv, W. Yu, Z.-W. Mao, L.-S. Wan and Z.-K. Xu, *ACS Appl. Mater. Interfaces*, 2014, **6**, 22400–22407.
6 J.-C. Hong, J.-H. Park, C. Chun and D.-Y. Kim, *Adv. Funct. Mater.*, 2007, **17**, 2462–2469.
7 T. Cassagneau and F. Caruso, *Adv. Mater.*, 2002, **14**, 1837–1841.
8 D. Beattie, K. H. Wong, C. Williams, L. A. Poole-Warren, T. P. Davis, C. Barner-Kowollik and M. H. Stenzel, *Biomacromolecules*, 2006, **7**, 1072–1082.
9 A. Sanz de Leon, J. Rodriguez-Hernandez and A. L. Cortajarena, *Biomaterials*, 2013, **34**, 1453–1460.
10 M. Du, P. Zhu, X. Yan, Y. Su, W. Song and J. Li, *Chem. Eur. J.*, 2011, **17**, 4238–4245.
11 B. You, L. Shi, N. Wen, X. Liu, L. Wu and J. Zi, *Macromolecules*, 2008, **41**, 6624–6626.
12 C. Li, G. Hong, H. Yu and L. Qi, *Chem. Mater.*, 2010, **22**, 3206–3211.

13 Y. S. Shin, C. M. Wang and G. L. Exarhos, *Adv. Mater.*, 2005, **17**, 73–77.
14 M. Xue, W. Xiao and Z. Zhang, *Adv. Mater.*, 2008, **20**, 439–442.
15 L. Santos, P. Martin, J. Ghilane, P.-C. Lacaze, H. Randriamahazaka, L. M. Abrantes and J.-C. Lacroix, *Electrochem. Commun.*, 2010, **12**, 872–875.
16 T. Pietsch, N. Gindy and A. Fahmi, *Soft Matter*, 2009, **5**, 2188–2197.
17 R. L. Luo, T. H. Young and Y. M. Sun, *Polymer*, 2003, **44**, 157–166.
18 Y. Zhang, H. Ding, S. Wei, S. Liu, Y. Wang and F.-S. Xiao, *J. Porous Mater.*, 2010, **17**, 693–698.
19 P. Escalé, L. Rubatat, L. Billon and M. Save, *Eur. Polym. J.*, 2012, **48**, 1001–1025.
20 A. Muñoz-Bonilla, M. Fernández-García and J. Rodríguez-Hernández, *Prog. Polym. Sci.*, 2014, **39**, 510–554.
21 T. G. Drummond, M. G. Hill and J. K. Barton, *Nat. Biotechnol.*, 2003, **21**, 1192–1199.
22 M. Schena, D. Shalon, R. W. Davis and P. O. Brown, *Science*, 1995, **270**, 467–470.
23 K. Keren, R. S. Berman, E. Buchstab, U. Sivan and E. Braun, *Science*, 2003, **302**, 1380–1382.
24 T. Sun, G. Qing, B. Su and L. Jiang, *Chem. Soc. Rev.*, 2011, **40**, 2909–2921.
25 W.-X. Zhang, L.-S. Wan, X.-L. Meng, J.-W. Li, B.-B. Ke, P.-C. Chen and Z.-K. Xu, *Soft Matter*, 2011, **7**, 4221–4227.
26 J.-T. Wu, T.-P. Sun, C.-W. Huang, C.-T. Su, C.-Y. Wu, S.-Y. Yeh, D.-K. Yang, L.-C. Chen, S.-T. Ding and H.-Y. Chen, *Biomater. Sci.*, 2015, 1266–1269.
27 A. Gefen, *Cellular and Biomolecular Mechanics and Mechanobiology*, Springer, Berlin, 2013.
28 D. Joester, M. Losson, R. Pugin, H. Heinzelmann, E. Walter, H. P. Merkle and F. Diederich, *Angew. Chem., Int. Ed.*, 2003, **42**, 1486–1490.
29 S. P. Jones, N. P. Gabrielson, D. W. Pack and D. K. Smith, *Chem. Commun.*, 2008, 4700–4702, DOI: 10.1039/b811852c.
30 S. Malhotra, H. Bauer, A. Tschiche, A. M. Staedtler, A. Mohr, M. Calderon, V. S. Parmar, L. Hoeke, S. Sharbati, R. Einspanier and R. Haag, *Biomacromolecules*, 2012, **13**, 3087–3098.
31 A. Tschiche, A. M. Staedtler, S. Malhotra, H. Bauer, C. Boettcher, S. Sharbati, M. Calderon, M. Koch, T. M. Zollner, A. Barnard, D. K. Smith, R. Einspanier, N. Schmidt and R. Haag, *J. Mater. Chem. B*, 2014, **2**, 2153–2167.
32 A. Tschiche, S. Malhotra and R. Haag, *Nanomedicine*, 2014, **9**, 667–693.
33 M. Calderon, M. A. Quadir, S. K. Sharma and R. Haag, *Adv. Mater.*, 2010, **22**, 190–218.
34 M. Martinelli, M. Calderon, C. I. Alvarez and M. C. Strumia, *React. Funct. Polym.*, 2007, **67**, 1018–1026.
35 R. Haag and F. Kratz, *Angew. Chem., Int. Ed.*, 2006, **45**, 1198–1215.
36 S. Malhotra, M. Calderon, A. K. Prasad, V. S. Parmar and R. Haag, *Org. Biomol. Chem.*, 2010, **8**, 2228–2237.
37 C. A. Bell, Z. Jia, S. Perrier and M. J. Monteiro, *J. Polym. Sci., Part A: Polym. Chem.*, 2011, **49**, 4539–4548.
38 M. H. Stenzel, *Aust. J. Chem.*, 2002, **55**, 239–243.
39 Y. Xue, S.-S. Zhang, K. Cui, J. Huang, Q.-L. Zhao, P. Lan, S.-K. Cao and Z. Ma, *RSC Adv.*, 2015, **5**, 7090–7097.
40 J.-F. Lutz, H. G. Börner and K. Weichenhan, *Macromol. Rapid Commun.*, 2005, **26**, 514–518.
41 P. L. Golas, N. V. Tsarevsky, B. S. Sumerlin and K. Matyjaszewski, *Macromolecules*, 2006, **39**, 6451–6457.
42 A. S. De León, S. Malhotra, M. Molina, R. Haag, M. Calderón, J. Rodríguez-Hernández and A. Muñoz-Bonilla, *J. Colloid Interface Sci.*, 2015, **440**, 263–271.
43 X. Xiong, M. Lin, W. Zou and X. Liu, *React. Funct. Polym.*, 2011, **71**, 964–971.
44 B. Jachimska and A. Pajor, *Bioelectrochemistry*, 2012, **87**, 138–146.
45 J. Fritz, E. B. Cooper, S. Gaudet, P. K. Sorger and S. R. Manalis, *Proc. Natl. Acad. Sci. U. S. A.*, 2002, **99**, 14142–14146.

